Influence of silicon on oxidation behaviour of Fe-Mn-Al and Fe-Mn alloys

F. FELLI, U. BERNABAI and M. CAVALLINI, Dipartimento ICMMPM, Università di Roma "La Sapienza", Rome, Italy

Abstract

A study was made of how the oxidation resistance in air of Fe-Mn-Al-C and Fe-Mn-C alloys at high temperatures is affected by the addition of small amounts, up to 3%, of silicon. An alloy containg 28% manganese, 8% aluminium, 2.4% silicon and 1% carbon showed good behaviour up to 950°C, with a weight increase of less than 1 mgcm^{-2} after 170 hours of testing at constant temperature. As the silicon content fell there is an appreciable reduction in the limiting temperature for acceptable resistance. The alloys without aluminium already showed considerable oxidability at 600°C. Oxide formation mechanisms were examined as a function of time and temperature, with thermogravimetric tests and ESCA and EDS analyses.

Riassunto

Influenza del silicio sul comportamento all'ossidazione di leghe Fe-Mn-Al e Fe-Mn

È stata studiata l'influenza di piccole aggiunte (fino a 3%) di silicio su leghe Fe-Mn-Al-C e Fe-Mn-C per quanto riguarda la resistenza all'ossidazione in aria ad alte temperature. La lega contenente 28% di manganese, 8% di alluminio, 2,4% di silicio ed 1% di carbonio ha mostrato un buon comportamento fino a 950°C, con un aumento di peso inferiore ad 1 mgcm^{-2} dopo 170 ore in prove isotermiche. Al diminuire del tenore di silicio diminuisce sensibilmente la temperatura limite di resistenza accettabile. In assenza di alluminio, già a 600°C le leghe presentano notevole ossidabilità. Sono stati esaminati i meccanismi di formazione degli ossidi in funzione del tempo e della temperatura con prove termogravimetriche e analisi ESCA ed EDS.

Introduction

Manganese-aluminium steels (20-32% Mn, 7-10% Al, 1% C) with a predominantly austenitic structure are currently arousing considerable interest (1), both because that structure is obtained without the aid of nickel and also because they give promise of resistance to the environment with chromium replaced by aluminium. Tests for resistance in reducing sulphide atmospheres (H_2 + 1% H_2S) at 700° and 800°C have given excellent results (2). The presence of silicon in alloys for that purpose is currently regarded with suspicion. Tests at 750°C in mixtures of fused sulphur salts and sulphate-chloride mixtures, therefore in an oxidizing sulphur atmosphere, have shown the important role of manganese associated with aluminium (3, 4). However, the material has shown better resistance to reducing sulphur environments than to oxidizing ones. These alloys have not given clearly promising results in corrosion tests in aqueous solutions (5).

Earlier tests of the air oxidation behaviour of alloys of this type (6) have indicated the possibility of achieving satisfactory resistance at temperatures higher than 700°C – a by no means negligible objective for a steel devoid of strategic or critical elements such as chromium or nickel (Figure 1 and Table 1). Those tests revealed that alloy A (Fe-20Mn-9Al-1C) satisfactorily resisted hot oxidation up to 700°C. Alloy F (Fe-27Mn-7.5Al-1.5Si-1C) behaved even better, forming manganese-rich oxide scale on the outside and aluminium scale near the matrix. Silicon seemed to

Fig. 1 - Temperature/weight curves of Alloys A and F in earlier work (6).

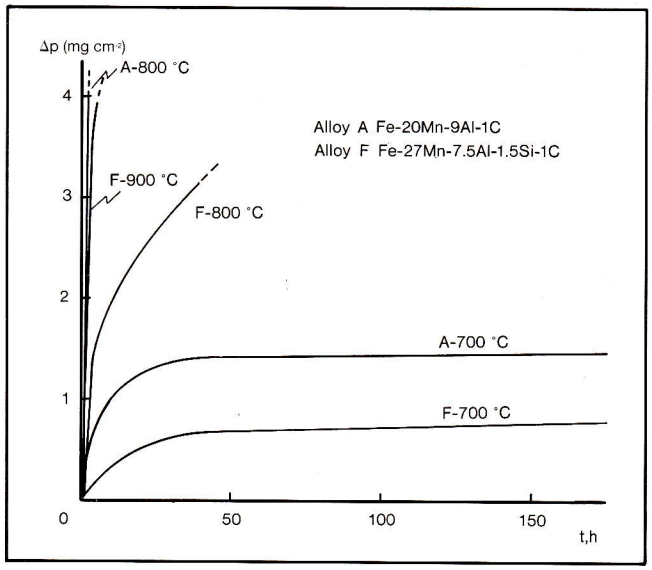

TABLE 1 - Composition (weight %) of Steels A and F in earlier work (6)

Code	Nominal composition	C	Mn	Al	Si	%ferrite
A	Fe-20Mn-9Al-1C	0.99	19.8	8.7	—	3
F	Fe-27Mn-7.5Al-1.5Si-1C	0.96	27.4	7.5	1.5	2

TABLE 2 - Composition (weight %) of steels in present work

Code	Nominal composition	C	Mn	Al	Si	%ferrite
G	Fe-20Mn-6Al-1.7Si-1C	0.98	19.8	6.07	1.74	0.5
H	Fe-28Mn-8Al-2.4Si-1C	0.92	27.9	7.96	2.36	22
I	Fe-20Mn-1.6Si-1C	1.05	19.9	—	1.63	0
L	Fe-27Mn-3Si-1C	0.93	27.4	—	3.07	0.8

have a particularly beneficial action, and it was also evident that a manganese content of up to about 19%, in keeping with the maintenance of an austenitic structure, likewise helped to improve resistance.
On the basis of those indications the alloys for the present work were prepared to the following criteria:

a) Partial replacement of aluminium by silicon in Alloy A (Fe-20Mn-9Al-1C).

b) Higher silicon in Alloy F (Fe-27Mn-7.5Al-1.5Si-1C).

c)) Total removal of aluminium from both alloys and replacement by a silicon content in keeping with ingot rolling capabilities.

The alloys used for the present work retain a carbon content of about 1% in order to ensure an austenitic structure; the addition of between 2% and 3% of silicon reduces the "gammagenous" effect of manganese (7).
The objects of this further experimental investigation were to provide a deeper understanding of the mechanisms controlling the formation of the various types of more or less protective oxide; to impede the growth of iron oxides in favour of manganese-rich mixed oxides, offering greater protection, or better still, in favour of those with a high alumina content having good adherence to the metal substrate; and hence to improve the air oxidation behaviour of the alloys at higher temperatures.

Materials and methods

Table 2 shows the compositions of the alloys. They were melted in an argon atmosphere, cast as 45 × 150 × 300 mm ingots, and rolled into 5 mm sheets. Rolling was done at between 900° and 1100°C and was followed by annealing at 1050°C for 30 minutes and then by quenching in water to prevent carbide precipitation, except for Steel H, which needed to be air-hardened. The ferrite content was measured with a Fischer Ferrit-Messer equipment.
Test pieces measuring 20 × 20 × 2 mm were taken from the sheets and polished up to 1 μm alumina paste.

Fig. 2 - Temperature/weight curves of Alloys I (on left) and L (on right).

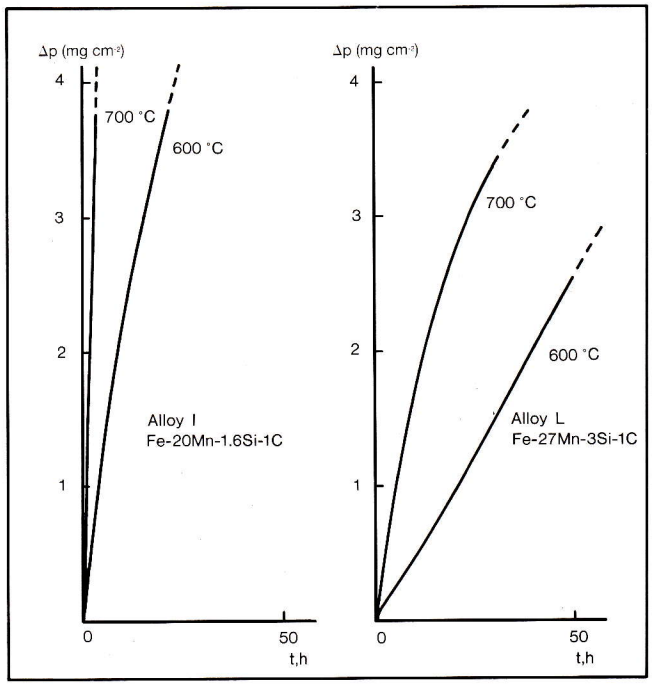

The hot oxidation tests were conducted in air and the increases in weight were recorded continuously by a Cahn 1000 thermobalance at temperatures between 600° and 1000°C for periods up to about 170 hours. In the figures that follow the temperature/weight curves were plotted with their average values when measurable deviations occurred in the experimental process, or with dispersion ranges when that was not possible. The analyses on oxidized samples were done with a scanning electron microscope and EDS analyser. The evolution of the composition in the early stages of oxidation was monitored by ESCA spectrometry (VG 3) on small samples oxidized for short periods.

Results

Temperature/weight curves

Figure 2 plots the results of the oxidation tests at

constant temperatures of 600° and 700°C for Alloys I and L (no aluminium). The data show that the materials can be oxidized considerably and that without aluminium no protective scale is formed. Sample L, with higher manganese and silicon contents, shows a slower oxidation rate than Sample I. Both materials displayed marked spalling of the scale when the specimen was cooled.

Figure 3 plots the results of the oxidation tests at constant temperature for Alloy G (Fe-20Mn-6Al-1.7Si-1C) in the temperature range 700-800°C. Up to 750°C the curves show a logarithmic trend, whereas at 800°C there is already massive oxidation in the first 24 hours, and a subsequent trend to a lower oxidation rate, but spalling is still present on cooling.

Figure 4 plots the results for Alloy H (Fe-28Mn-8Al-2.4Si-1C) in the 750° to 1000°C range. Up to 950°C the curves are near parabolic with end values for weight increase of not more than about 1 mgcm^{-2} for times of 170 hours. The curves from 800° to 950°C fall in the dispersion range shown in the figure without precise correspondence between increases in weight and temperature. At 1000°C, on the other hand, oxidation is rapid, with spalling on cooling.

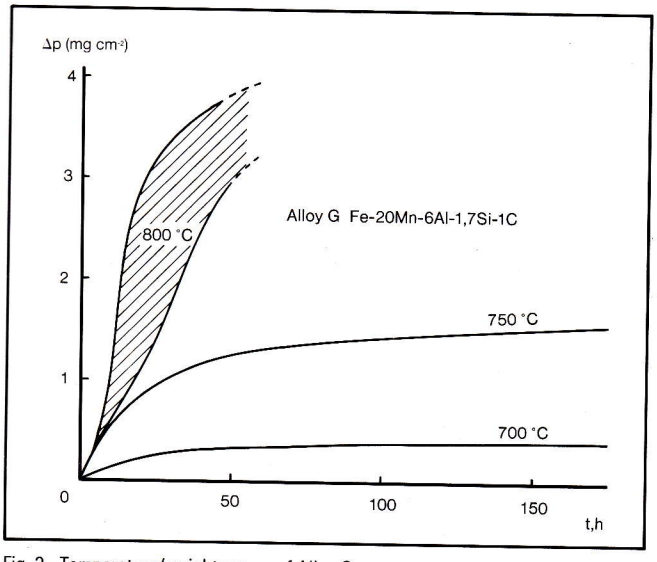

Fig. 3 - Temperature/weight curves of Alloy G.

ESCA analysis

Figures 5-7 show the atomic concentration maps for the various elements that make the oxides in the early phases of oxidation, as detected by ESCA analysis. That analysis reveals only the overall composition of the outermost part of the oxide layer (2-5 nm) and should therefore be taken in conjunction with the EDS analyses for much greater thicknesses (2 µm or more) and the EDS line analyses done on sections of the oxidized samples.

Figure 5 relates to Sample L (Fe-27Mn-3Si-1C) for times up to 60 minutes at 600°C. Massive oxidation of manganese in preference to iron is evident; silicon does not appear in these early stages of oxidation. The preponderance of manganese over iron becomes ever

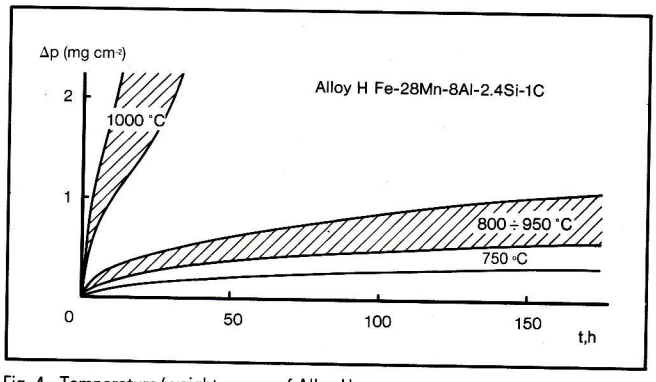

Fig. 4 - Temperature/weight curves of Alloy H.

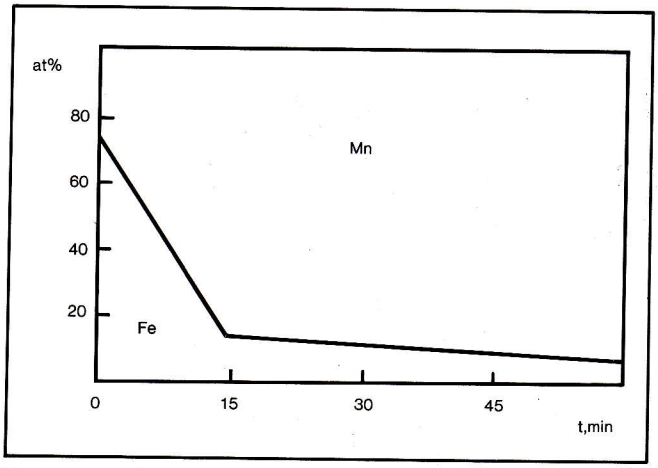

Fig. 5 - ESCA atomic composition of Alloy L oxidized at 600°C.

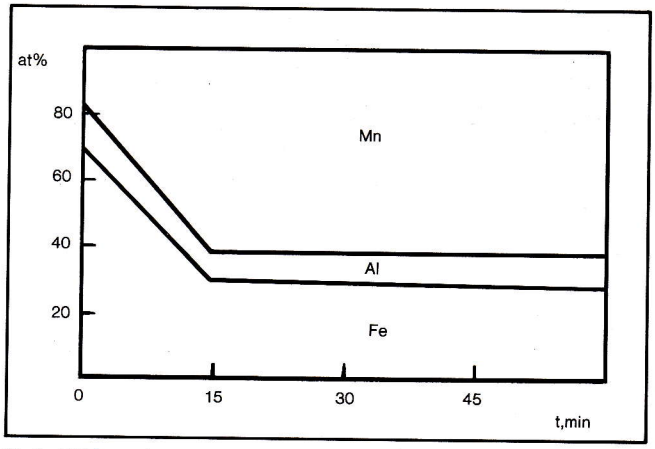

Fig. 6 - ESCA atomic composition of Alloy G oxidized at 700°C.

Fig. 7 - ESCA atomic composition of Alloy H oxidized at 800 to 1000°C.

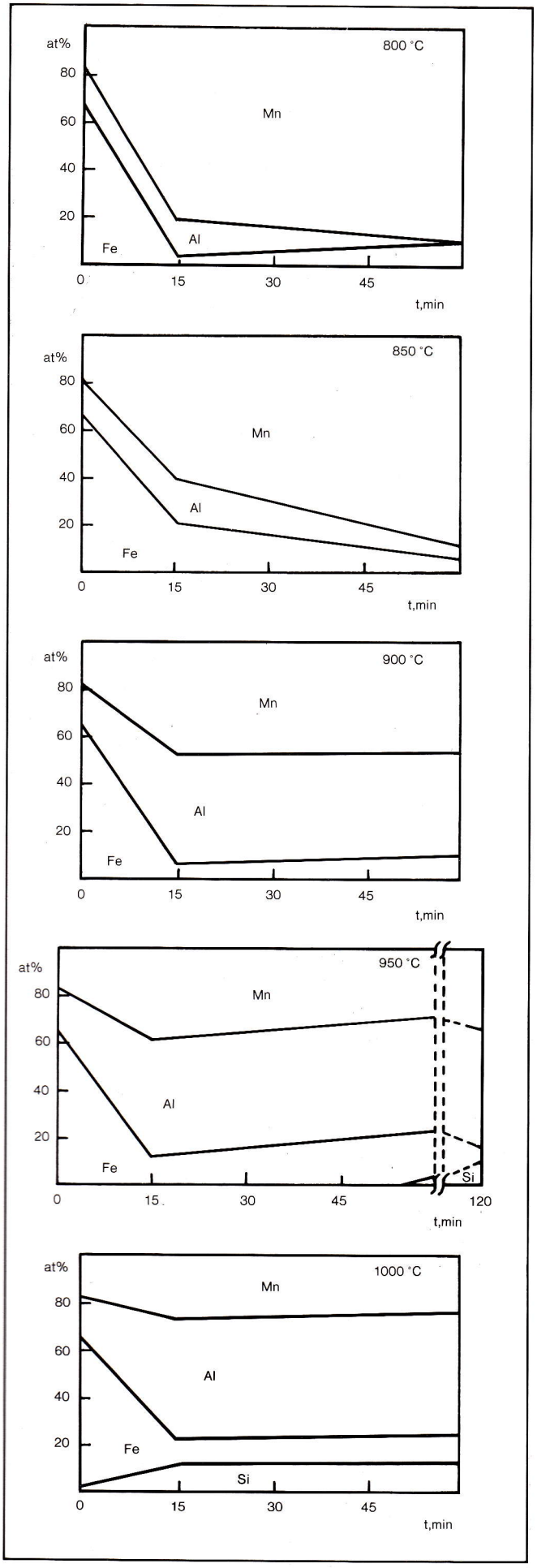

less marked as the surface layer of oxide is removed by ion bombardment; ESCA analysis then reveals that along with the preferential oxidation of manganese there is also surface segregation of that element in the oxide.

Figure 6 relates to Sample G (Fe-20Mn-6Al-1.7Si-1C) at 700°C and shows preferential oxidation of manganese and the presence of aluminium in proportions close to the nominal composition of the alloy.

Figure 7 shows the maps for Sample H (Fe-28Mn-8Al-2.4Si-1C) at temperatures of 800°, 850°, 900°, 950° and 1000°C for times up to one hour, with a spectrum taken also at two hours for 950°C. At the lower temperatures (800° and 850°C) there is preferential oxidation of manganese at the expense of iron and aluminium; from 900°C upwards aluminium predominates over manganese, increasingly so as the test temperature is increased. Only after two hours at 950°C or in the test at 1000°C does silicon appear at the surface.

Oxide morphology

The oxidation process and the formation of oxide surface scale were studied from a morphological standpoint with a scanning electron microscope (SEM), to provide detailed documentation of the evolution of the composition with numerous EDS spot analyses.

Samples I and L show a thick scale, rich in iron and manganese-base spinels, with a strong tendency to spall on cooling.

Sample G (Fe-20Mn-6Al-1.7Si-1C), oxidized at 700° for 170 hours (Figure 8), shows a largely compact scale interrupted by a few individual spinel formations (Mn/Fe ratio between 2 and 4) with a higher growth rate outwards without spreading on the surface. At higher

Fig. 8 - Surface aspect under SEM of Alloy G oxidized for 170 hours at 700°C.

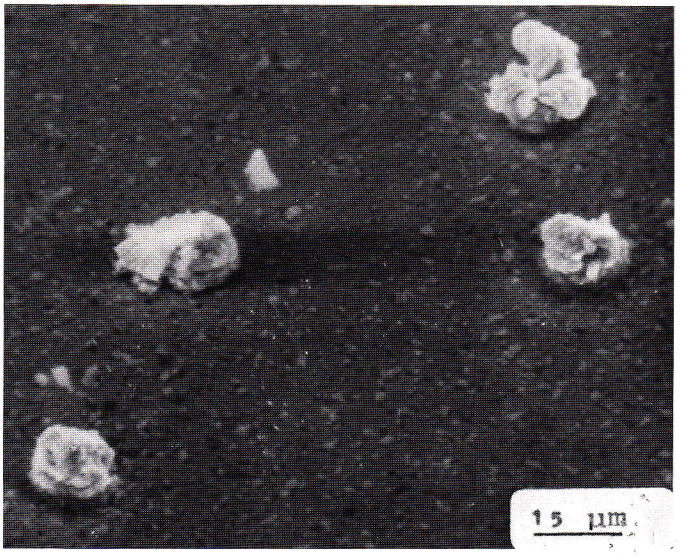

temperatures fast-growing spinel formation is enhanced and determines spalling on cooling.
The behaviour of Sample H (Fe-28Mn-8Al-2.4Si-1C) varies according to the oxidation time and temperature. In view of the great interest of the temperature/weight results for this sample, a fuller documentation is given in regard to the morphological development of the oxides, both for short times (see ESCA analysis in Figure 7) and for longer times. It was noted that oxide nuclei appeared in fair numbers at the grain boundaries (Figure 9) after 15 minutes at 800°C. Subsequently, after 60 minutes at the same temperature, it was noted that oxide growth at grain boundaries was inhibited and concurrently there was growth of mixed oxides, very rich in manganese, finely dispersed over the whole surface inside the grain (Figure 10). At higher temperatures (1000°C, 15 min), on the other hand, it was noted that there was formation of a matrix surface structure inside the grains in "reticulate" form. The geometric appearance of the meshes suggests that surface voids are involved. Oxide outgrowths at grain boundaries remain inhibited during scale formation. At the same time, a layer of alumina-rich oxide (about 50% aluminium by weight – see Figure 11) appears. With increasing time (60 min) there are localized breakdowns of the oxide film, due to the formation of fast-growing spinel, rich in iron and manganese.
For long oxidation times, again for Sample H, in the 750°-850°C temperature range we find the same characteristic "reticulate" surface morphology of voids exposed by spalling (Figure 12). Sporadically there appear very thin layers, transparent to the secondary electrons captured in the electronic image; they are composed principally of alumina and contain no silicon. Figure 13 shows the line analysis done on a section of the sample in Figure 12: two layers are noted, an outer one involving manganese, iron and aluminium, and an

Fig. 9 - Surface aspect under SEM of Alloy H oxidized for 15 minutes at 800°C.

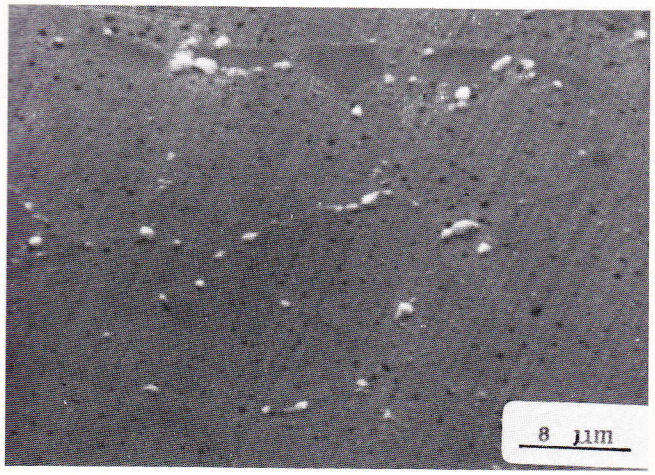

Fig. 10 - Surface aspect under SEM of Alloy H oxidized for 60 minutes at 800°C.

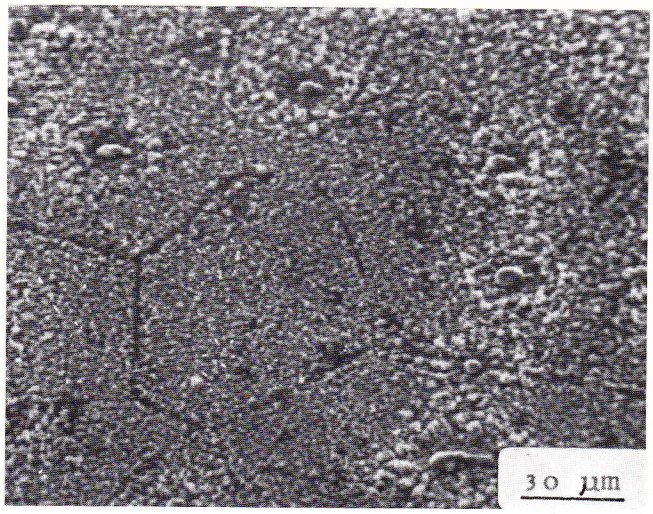

Fig. 11 - Surface aspect under SEM of Alloy H oxidized for 15 minutes at 1000°C.

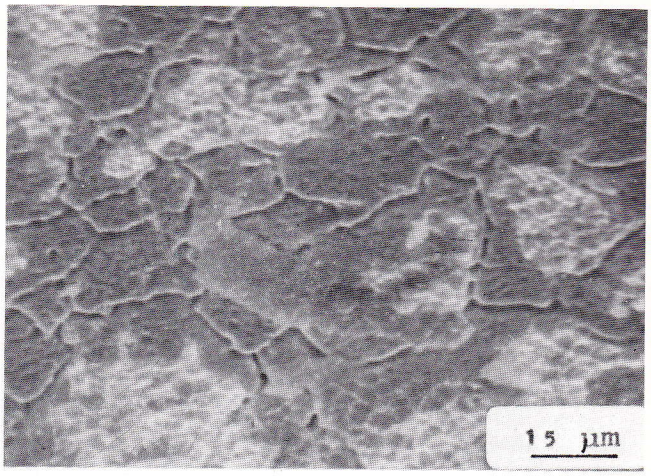

Fig. 12 - Surface aspect under SEM of Alloy H oxidized for 170 hours at 800°C.

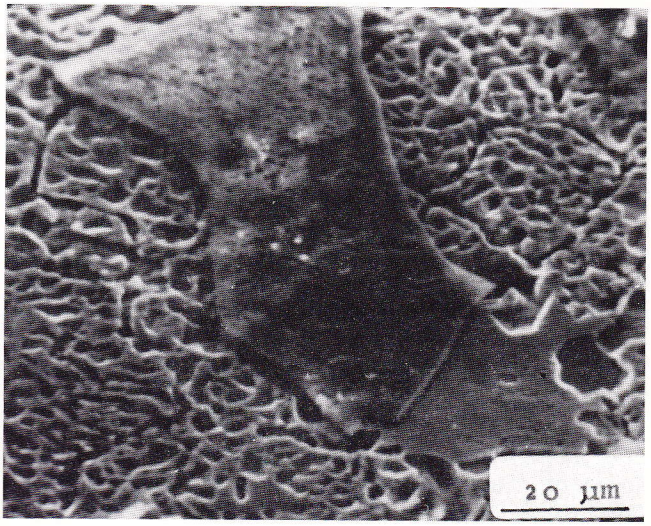

inner one with a high aluminium content opposite a minimum of iron and manganese, whereas silicon appears only at the innermost part, opposite the aluminium peak.
At higher temperatures (850°-950°C) the above reticulate structure is absent. The oxide film consists in a subscale (Zone B in Figure 14) partly covered by an inhomogeneous scale of oxides richer in alumina (Zone A in Figure 14).
The line analysis in Figure 15 of a section through an A zone of Figure 14 shows, starting from the outer surface, a first layer rich in aluminium, a second rich in manganese, and a third, the innermost, very rich in aluminium. Silicon mostly remains low, but an enrichment peak can be clearly identified at the matrix-oxide interface. At 1000°C the morphology is inhomogeneous; zones in which the scale is protective, of the type formed at 950°C, are interspersed with zones of fast-growing oxides with a tendency to spalling.

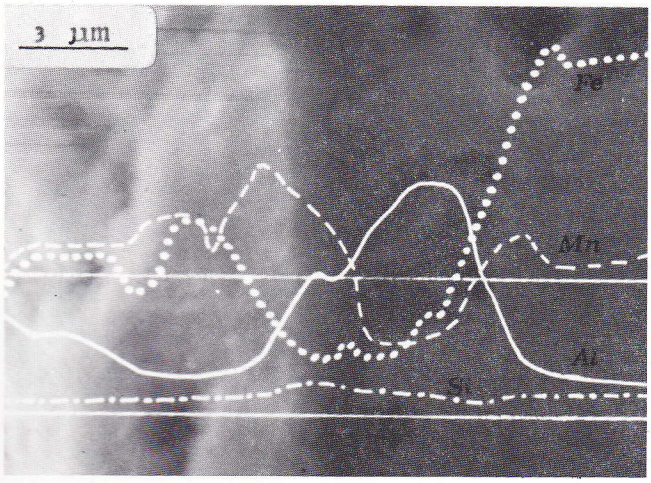

Fig. 13 - Section of sample in preceding figure with EDS line analysis of Fe, Mn, Al and Si.

Discussion

Thermodynamically speaking, the oxygen affinities of aluminium, silicon, manganese and iron are on a descending scale in that order, but kinetically speaking the surface analyses and metallographic data indicate that there are mechanisms of diffusion and selective oxidation that involve obvious departures from thermodynamic behaviour. Oxidation rates are governed, moment by moment, by interaction between the alloying elements, depending on temperature, time and local activity.
The results of the present work, considered in conjunction with those of the earlier work we have mentioned (6) (see also Figure 1), provide a basis for discussion allowing the following points to be made:

1) Aluminium's inability to form very pure protective films of alumina, whereas that possibility has been observed, for example, in ferritic Cr-Al steels (8). Aluminium, however, is involved in the formation of scale and governs its growth at various levels.
2) The formation of manganese-base spinel, in which the predominance of manganese over iron depends on the presence of silicon, which control the mechanism on diffusion through the scale at the matrix-scale interface. A higher content of manganese at the expense of iron should be regarded as a more favourable condition for controlling the oxidation process, as the oxide is then less porous and the result is an improved barrier action that allows the aluminium to play a part in forming the scale, even though this is only partly protective.

Silicon's influence on the Fe/Mn ratio of the mixed oxides that are formed emerges clearly from a

Fig. 14 - Surface aspect under SEM of Alloy H oxidized for 170 hours at 900°C, at two different magnifications. The A zones are rich in aluminium, the B zones in manganese.

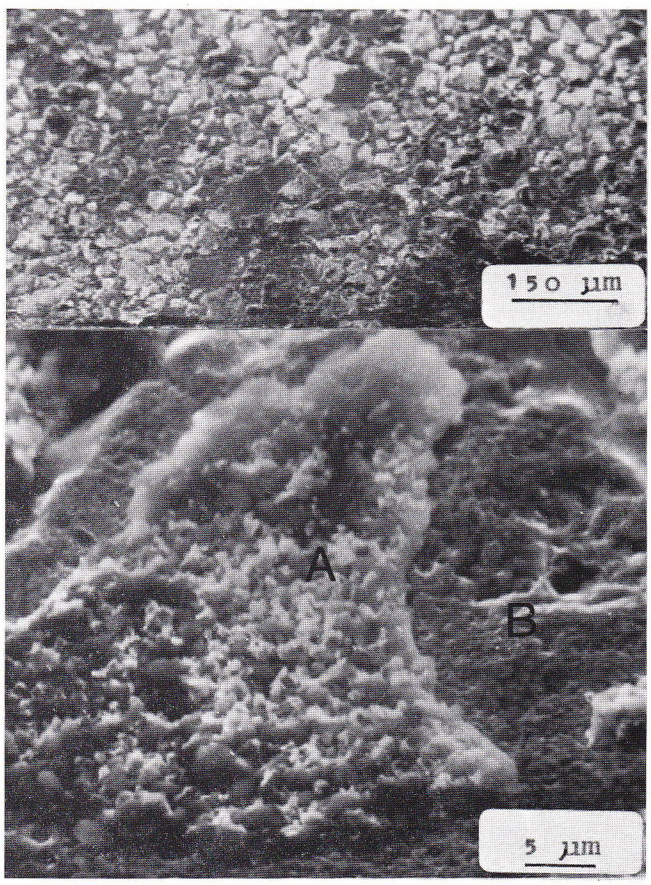

comparison of the behaviour of Alloy G in the present work (Fe-20Mn-6Al-1.7Si-1C) with that of Alloy A of the earlier work (Fe-20Mh-9Al-1C). After 100 hours at 700°C the weight increases are 0.3 $mgcm^{-2}$ for Sample G and 1.5 $mgcm^{-2}$ for Sample A (Figure 1 and 3); after 4 hours at 800°C the figures are 0.5 and 5 $mgcm^{-2}$ respectively.
In considering silicon's action in the presence of aluminium the following experimental evidence must be taken into account:

1) ESCA analysis did not detect silicon at the outer surface of the oxide in the early stages of oxidation, except at 1000°C or after two hours at 950°C.
2) At the lower temperatures, silicon enrichment is identified in the subscale; its influence on the mechanism of oxide scale formation finds an explanation in the diffusion phenomenon involved. It is known that silicon has a low diffusion rate in oxide layers (9) and so this brings about enrichment at the interface with the metal, where the silicon can exercise control of cation diffusivity.

It is also noted that this control seems to be exerted more on iron than on aluminium and manganese. Other authors (10, 11) have also recently found, in microprobe analysis profiles, that manganese has greater capacity than iron to diffuse through a layer of silicon oxide; in addition, Atkinson and Gardner (12) had already shown the low diffusivity of Fe^{3+} through a layer of amorphous silica (at about 850°C $D = 10^{-15}\ cm^2\ s^{-1}$). It can be hypothesized that in the presence of Fe^{2+} compact layers of fayalite may be formed by interaction with the silica. This filter action exerted by silicon at the metal-oxide interface therefore means that the scale is enriched with aluminium or manganese oxides, or both, and this helps to lower the oxidation rate.
The temperature/weight results of the oxidation tests at 800° to 950°C (Figure 4) were represented with a dispersion range suggesting that rate control, though remaining of the same magnitude, operates at several levels of the oxide layer and with different mechanisms according to the temperature. As for the lower temperature in the range, let us consider the ESCA analysis in Figure 7 and the EDS analysis profile in Figure 13: they give evidence of the initial formation of a layer of manganese-rich mixed oxides under which gradually develops a subscale that is being enriched in aluminium and which also shows traces of silicon oxides at the longest oxidation times.
At 900°C or higher the ESCA analysis reveals an aluminium-rich oxide right from the early stages, and silicon oxides also appear for times around two hours at 950°C. At long exposure times (170 hours) scale morphology appears transformed as compared with the lower temperatures: on the outside (Figure 14) a thick layer rich in aluminium oxide appears (Zone A) over an underlying subscale (Zone B). Silicon and

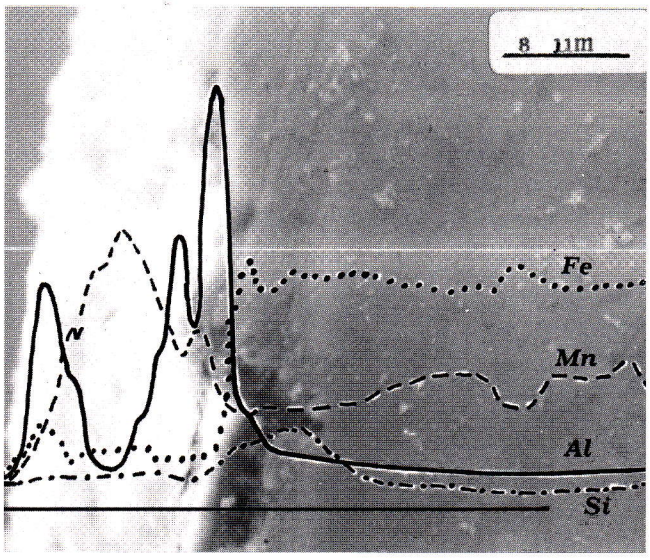

Fig. 15 - Section of an A zone of sample in preceding figure with EDS line analysis of Fe, Mn, Al and Si.

aluminium, the most protective elements, are found from the start in the uppermost layers. The EDS profile (Figure 15) done on the section of Sample H exposed for 170 hours at 900°C shows aluminium both on the outside and in the subscale, with manganese predominating over iron in the intermediate zone.
At 1000°C oxide formation is exactly similar to that at 950°C, but with long times the system ceases to be capable of controlling the formation rate and catastrophic oxidation ensues.
In connection with what has been said about the Fe-Mn-Al-Si alloys, where the formation of surface scale is concerned, it will be noted that the grain boundaries make but a slight contribution or may even have an inhibiting effect. In other types of alloy the greater diffusivity of alloying elements at the grain boundaries usually has the results that oxidation of the various elements ceases to be selective along those edges. The rule is confirmed in the earliest stages of exposure in the present case (Figure 9), since immediately afterwards blocking occurs at the boundaries (Figure 10) and has repercussions on the morphology of the mixed oxides (Figure 12), in which the outline of the grain boundaries can be seen even after long exposure times (170 hours).
Without aluminium (Alloys I and L) there is no actual protective mechanism at the test temperatures and the scale is not adherent, even though in the case of the highest silicon content (3% in Alloy L) there is a hint of inflexion in the temperature/weight curves (Figure 2). It must be considered, because of the mechanism explained, that a higher silicon content encourages the oxidation of manganese in preference to iron; on the other hand, the difficulty in working materials

containing more than 3% silicon by plastic deformation sets a pratical limitation on the use of higher percentages.

Conclusions

Fe-Mn-Al-Si alloys look particularly promising in their resistance to high-temperature oxidation in air, showing themselves clearly better than Fe-Mn-Al alloys. The Fe-28Mn-8Al-2.4Si-1C alloy showed the best behaviour for long periods at constant temperatures up to 950°C, without excessive oxide growth and spalling when cooled. The following hypotheses seem capable of explaining the mechanisms through which that behaviour is possible:

1) Formation of a protective film rich in aluminium, manganese, or both, with a low iron content.
2) Silicon enrichment at the oxide-matrix interface, with a filter effect on cation diffusion of the oxide-forming elements.

Acknowledgements

The work was carried out with an M.P.I. research grant. The authors are grateful to the Centro Sperimentale Metallurgico (CSM) for supplying the experimental alloys, Professor C. Furlani for the ESCA analyses, and Professor G. Violi for discussing the work.

REFERENCES

(1) Banerji, S.K. The 1982 status on Fe-Mn-Al steels. In a Report of Foote Mineral Company, Exton, PA 19341 (1982).

(2) Tomas, P. Elements essential to high temperature sulphidation resistant iron-based alloys. In ***Proc. 35th Annual Conf. of the Australasian Inst. of Metals,*** *Sydney, Australia, May (1982), pp. 90-98.*

(3) Bombara, G., F. Felli, and U. Bernabai. Investigation into the hot salt corrosion of Cr-Al, Cr-Ni-Mn and Mn-Al steel. ***Werkst, Korrosion., 33*** *(1982), 491-497.*

(4) Bernabai, U., and F. Felli. The role of Cr, Al and Mn in the resistance of refractory steels to hot salt corrosion from combustion deposits. ***Metall. Sci. Technol. 3*** *(1985), 39-45.*

(5) Cavallini, M., F. Felli, R. Fratesi, and F. Veniali. Aqueous solution corrosion behaviour of "poor man" high manganese-aluminium steels. ***Werkst. Korros., 33*** *(1982) 281-284.*

(6) Cavallini, M., F. Felli, R. Fratesi, and F. Veniali. High temperature air oxidation behaviour of "poor man" high manganese-aluminum steels. ***Werkst. Korros., 33*** *(1982) 386-390.*

(7) Sauer, J.P., R.A. Rapp, and J.P. Hirth. Oxidation of iron-manganese-aluminum alloys at 850 and 1000°C. ***Oxid. Met., 18*** *(1982) 285-294.*

(8) Bernabai, U., M. Cavallini, S. Fortunati, and A. Tamba. Ossidazione in aria ad alta temperatura di acciai ferritici Fe-Cr-Al addizionati con terre rare. ***Boll. Tecn. Finsider, 395*** *(1982) 180-191.*

(9) Kubaschewski, O., and B.E. Hopkins. In ***Oxidation of metals and alloys.,*** *Butterworths, London, 1962.*

(10) Lobb, R.C., and H.E. Evans. An evaluation of the effect of surface chromium concentration on the oxidation of a stainless steel. ***Corros. Sci., 23*** *(1983), 55-73.*

(11) Bennett, M.J., M.R. Houlton, and R.W.M. Hawes. The improvement by CVD silica coating of the oxidation behaviour of a 20% Cr/25% Ni niobium stabilized stainless steel in carbon dioxide ***Corros. Sci., 22*** *(1982) 111-133.*

(12) Atkinson, A., and J.W. Gardner. The diffusion of Fe^{3+} in amorphous SiO_2 and the protective properties of SiO_2 layers. ***Corros. Sci., 21*** *(1981) 49-58.*